
Araştırma Makalesi / Research Article

Comparison of Mechanical Properties of Samples Fabricated by Stereolithography and Fused Deposition Modelling

M. Said BAYRAKLILAR¹, Abdulkadir BULDU², M. Tayyip KOCAK³, Osman ULKIR^{4*},
Melih KUNCAN⁵

¹Department of Civil Engineering, Faculty of Engineering, Siirt University, Siirt, Turkey,
ORCID ID: <https://orcid.org/0000-0002-5365-4441>, said.bayraklilar@siirt.edu.tr

²Department of Electrical and Electronics Engineering, Faculty of Engineering, Siirt University, Siirt, Turkey
ORCID ID: <https://orcid.org/0000-0002-9161-4862>, abdulcadir.buldu@siirt.edu.tr

³Department of Software Engineering, Istanbul Health and Technology University, Istanbul, Turkey,
ORCID ID: <https://orcid.org/0000-0003-2276-2658>, muhammedtayyipkocak@gmail.com

⁴Department of Electric and Energy, Technical Sciences Vocational School, Mus Alparslan University, Mus, Turkey,
ORCID ID: <https://orcid.org/0000-0002-1095-0160>, o.ulkir@alparslan.edu.tr

⁵Department of Electrical and Electronics Engineering, Faculty of Engineering, Siirt University, Siirt, Turkey,
ORCID ID: <https://orcid.org/0000-0002-9749-0418>, melihkuncan@siirt.edu.tr

Geliş/ Received: 13.09.2023;

Kabul / Accepted: 31.10.2023

ABSTRACT: Additive manufacturing (AM) technology has attracted significant attention with the rapid fabrication of 3D parts for various applications. The two most popular techniques in this technology, Fused Deposition Modelling (FDM) and Stereolithography (SLA), make it possible to produce functional parts with complex shapes quickly and cheaply. Determining the mechanical properties of the parts fabricated by these methods is important in terms of efficient operation in the relevant fields. In this study, forty-five test specimens were fabricated using three different polymer materials (UVR, PLA, and ABS) in SLA and FDM type 3D printers, including tensile, compression, and 3-point bending tests. Samples are printed at a 75% fill rate according to ASTM standards. Experimental studies were carried out to determine the mechanical properties of the samples. Among the samples, the highest strength values in tensile, compression and bending test samples made of UVR material were 60.39 MPa, 127.74 MPa and 118.35 MPa, respectively. In addition to mechanical properties, hardness, and SEM analyses were performed to examine the surface roughness, surface topography, and composition of the samples.

Keywords: Additive manufacturing, Compression test, Fused deposition modelling, Stereolithography, Tensile test, 3-point bending test.

*Sorumlu yazar / Corresponding author: o.ulkir@alparslan.edu.tr

Bu makaleye atıf yapmak için /To cite this article

Bayraklılar, M.S., Buldu, A., Kocak M.T., Ulkir, O., Kuncan, M. (2023). Comparison of Mechanical Properties of Samples Fabricated by Stereolithography and Fused Deposition Modelling Additive Manufacturing Methods. Journal of Materials and Mechatronics: A (JournalMM), 4(2), 475-491.

1. INTRODUCTION

Additive manufacturing (AM) produces objects directly from three-dimensional (3D) models by combining materials layer by layer. Appropriate application of AM can help to save fabrication time and cost, shorten the product development cycle, and increase fabrication capability and complexity (Singh et al., 2017). Thanks to its unique fabrication technique, AM is adopted in many industrial applications such as aerospace, automobile, automation, food, and pharmaceutical (Haleem and Javaid, 2019; Böcking and Tillman, 2019; Ble-Bail et al., 2020). The main additive manufacturing applications include rapid prototyping, rapid tooling, and rapid manufacturing. Much research is being done to improve the AM process by developing new fabrication technologies, evaluating environmental sustainability performance by performing cost analysis and evaluation, and improving printing accuracy and quality (Cheeser et al., 2019; Uludag et al., 2023). AM technologies are primarily applied for fit and function prototyping and tooling in the design and modeling phase. In such cases, the mechanical properties of prototypes or tools are very important (Shassere et al., 2019; Du Plessis et al., 2020). Because products must withstand high pressure from the rig or injection molding testing. It is important to determine these pressure data in tension, compression, and bending conditions before the product is used.

The distinguishing features of AM are often presented in the context of comparison with traditional manufacturing processes. The term "additive manufacturing" is ultimately defined by the American Testing and Materials Corporation (ASTM) F42 committee as a technique. AM techniques can be divided into seven categories according to the ASTM standard (Kawalkar et al., 2022): material extrusion, powder bed fusion, vat photopolymerization, material sputtering, binder sputtering, sheet lamination, and directed energy deposition (Li et al., 2020; Duman and Ozsoy, 2022). These processes include stereolithography (SLA) (Ertugrul et al., 2023), electron beam melting (EBM) (Galati et al., 2018) selective laser melting (SLM) (Cheng et al., 2016), fused deposition modelling (FDM) (Ozsoy et al., 2022), polyjet (Patpatiya et al., 2022), two photon polymerization (2PP) (Nguyen and Karayan, 2017) and digital light processing (DLP) (Chaudry et al., 2023) are also widely used in AM. In the current study, FDM, a material extrusion process, and SLA, a photo polymerization-based method, were preferred. These methods are the most preferred and researched technologies in the 3D printing process.

While various methods exist for the 3D printing process, FDM is a widely used methodology. In the FDM technique, the 3D printers used a thermoplastic type filament, which is heated until it reaches its melting temperature, then extruded layer by layer (Shi et al., 2021). The uninterrupted usability of the given material is made by using printing pieces in a layered manner. The heating element in the liquefier head is used to bring the filament to a semi-liquid phase, which is then extruded from the nozzle into the printing area to print the actual component. The most important task in this process is to melt the next layer before it solidifies since solidification before fusing can have a greater impact on other properties of the component. The most used raw materials in the FDM fabrication process are Acrylonitrile Butadiene Styrene (ABS), Polylactic Acid (PLA), Polycarbonate (PC), Polyethylene Terephthalate Glycol (PETG), and Thermoplastic Polyurethane (TPU) (De Leon et al., 2019; Yadav et al., 2020). Parts fabricated with FDM are suitable for detailed functional prototypes, durable fabrication tools, and low-volume fabrication. FDM is used in aviation, medicine, consumer goods, architecture, and automotive (Chohan et al., 2017; Kempin et al., 2017).

SLA is the first AM technology in which a liquid photosensitive resin is converted into a solid by selectively exposing it to an ultraviolet (UV) light (Prabhakar et al., 2021). The liquid-based materials used in the SLA process are complex chemical compounds specially designed for each SLA

printer. Both solid and powder-based materials used in SLA are polymers such as photopolymer resin, PLA, and ABS (Miedzinska et al., 2020). While SLA materials are fragile, toxic, or vulnerable to light exposure, recent developments gradually reduce these limitations. During the process, a thin layer of liquid in contact with UV light is solidified into the fabrication bed. When the process is complete, the fabrication bed is removed with the fabricated object attached to it; then, it is unbreakable and cleaned with alcohol-based chemicals. Depending on the material selection, the part is either post-treated with other chemicals or cured briefly under intense UV light (Kafle et al., 2021). SLA is widely used in the fabrication of medical prototypes and prosthetics, small and sensitive prototypes, optical parts and transparent fabrications, and dental fields (Dehurtevent et al., 2017; Mukhtarkhanov et al., 2020).

Many studies are carried out to determine and develop various properties of products fabricated with SLA and FDM methods (Heidari-Rarani et al., 2019; Camargo et al., 2019; Marsavina et al., 2022) Mercado-Colmenero et al., (Mercado-Colmenero et al., 2020) present numerical and experimental analysis of polymeric material PETG fabricated by FDM technology, aiming to obtain its mechanical characterization under uniaxial compression loads. Yadav et al., (Yadav et al., 2020) discussed the effects of material density, filler density, and extrusion temperature on the tensile strength of ABS, PETG, and multi-material test pieces. The multi-material is fabricated by layer-by-layer bonding of 50% ABS and 50% PETG in an FDM 3D printer. A total of 30 test pieces were printed according to ASTM D638-(IV) standard with different fill densities, extrusion temperatures, and material densities. In addition, the fill density and extrusion temperature are optimized to increase the tensile strength of the FDM fabrication units. Özsoy et al., (Özsoy et al., 2021) fabricated 36 test specimens, including two different polymer materials (PLA and ABS), tensile, compression tests, and 3-point bending tests, in the FDM-type printer. Chacón et al. (Chacón et al., 2017) aimed to characterize the effect of structure direction, layer thickness, and feed rate on the mechanical performance of PLA samples fabricated with a low-cost 3D printer.

Tensile and three-point bending tests were performed to determine the mechanical response of the printed samples. Due to the layer-by-layer fabrication, it was observed that the samples exhibited anisotropic behaviour, and vertical orientation showed the lowest mechanical properties. Regarding layer thickness and feed rate, it was determined that ductility decreased as the layer thickness and feed rate increased. The current study is aimed to compare the mechanical properties of the samples by producing tensile, compression, and bending tests with these three types of materials in SLA and FDM-based 3D printers. Thus, innovation will be added to the literature.

In this study, test samples were fabricated using three different polymer materials (UVR, PLA, and ABS) to examine the material properties of SLA and FDM 3D printing methods, which are AM methods. Test specimens were prepared according to ASTM standards for plastic materials. While UVR material was used in the SLA to produce the samples, PLA and ABS materials were used in the FDM. Forty-five test specimens were fabricated for each process parameter, including fifteen tensile, fifteen compressions, and fifteen bending tests.

2. MATERIALS AND METHODS

2.1 Materials

This section presents the types of 3D printers and materials used in the additive manufacturing process of the test samples whose mechanical properties will be examined. Since the samples will be fabricated by Stereolithography (SLA) and Fused Deposition Modelling (FDM) methods, two types

of printers were used. FDM-based 3D printing can be obtained from these printers with the printer in Figure 1a. Creality Ender 6 brand printer has a large print volume of 250x250x400 mm. In addition, the printing speed can reach 150 mm/s with 0.1 mm resolution. Printing with PLA, ABS, TPU, Nylon, HIPS, and conductive filament types is possible with the Creality printer. The slicing program named Cura was used for the printing process with this printer. SLA-based 3D printing is possible with the printer in Figure 1b. The FlashForge Foto 6.0 brand printer has a low print volume of 130x78x155 mm. However, finely detailed prints can be obtained in small volumes with high efficiency and precision. The printer has a pixel resolution of 2560x1620 and offers a print speed of 30 mm/h. The slicing program called Chitubox was used for the printing process with the printer. Ultraviolet light-sensitive fluid resin was used as the printing material in the Flashforge Photo 6.0 printer.

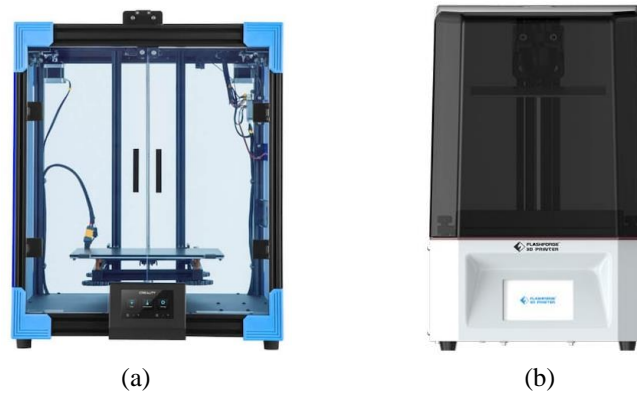


Figure 1. FDM and SLA type printers used in 3D fabrication (a) Creality Ender 6 (b) Flashforge Foto 6.0

Three materials were used to produce test samples: ABS, PLA, and UVR. PLA and ABS were used in filament form, while UVR was used in fluid form. ABS is a common thermoplastic polymer typically used for injection moulding applications. This engineering plastic is popular for its low cost of manufacture and ease of processing by the material's plastic manufacturers. ABS material is advantageous in various industries due to its properties such as structural strength and rigidity, chemical resistance, and excellent electrical insulation. However, it also brings restrictions due to its properties such as being damaged by sunlight and being dangerous when burned. PLA is a completely biodegradable thermoplastic polymer composed of renewable raw materials. Another advantage of using PLA filament is its environmentally friendly properties (Morão and De, 2019).

Table 1. Properties of ABS, PLA and UVR materials

| | Compression Temperature (°C) | Density (g/cm³) | Tensile Strength (MPa) | Elongation at Break (%) | Bending Strength (MPa) | Impact Strength (kJ/m²) |
|-----|-------------------------------------|-----------------------------------|-------------------------------|--------------------------------|-------------------------------|---|
| PLA | 180-215 | 1.24 | 65 | 28 | 92 | 6.8 |
| ABS | 210-230 | 1.04 | 40 | 40 | 75 | 7.6 |
| | Viscosity (mPa.s) | Density (g/cm³) | Tensile Strength (MPa) | Elongation at Break (%) | Wavelength (nm) | Hardness (D) |
| UVR | 150-200 | 1.25 | 52 | 20 | 405 | 84 |

As a biodegradable material made from renewable resources, it produces fewer emissions during the printing process compared to other materials. Among all 3D printing materials, PLA is part of the most popular materials used for additive manufacturing for filament fabrication. The UV resin material is viscous and is fabricated for 3D printing devices. The photopolymer-based resin

material has fast-drying properties after exposure to UV light. After curing, UV resin is non-stick, clear, yellowing, and scratch resistant. Recently, it has been used frequently in industrial applications and biomedical fields. Some technical specifications of ABS, PLA and UVR materials are given in Table 1 (Aloyaydi and Sivasankaran, 2020; Kim et al., 2007; Turan et al., 2022).

ASTM standard was preferred for sizing test samples. The technical drawing and dimensions of the samples are shown in Figure 2. ASTM D638-14, ASTM D695, and ASTM D790 standards were used for tensile, compression, and 3-point bending tests, respectively (Laureto and Pearce, 2018; Salman et al., 2015; Ishak et al., 2010). The samples were fabricated in the dimensions shown in Figure 2 and with a thickness of 3.20 mm. Solid models of the samples were made in 3D with SolidWorks software within the framework of the specified dimensions.

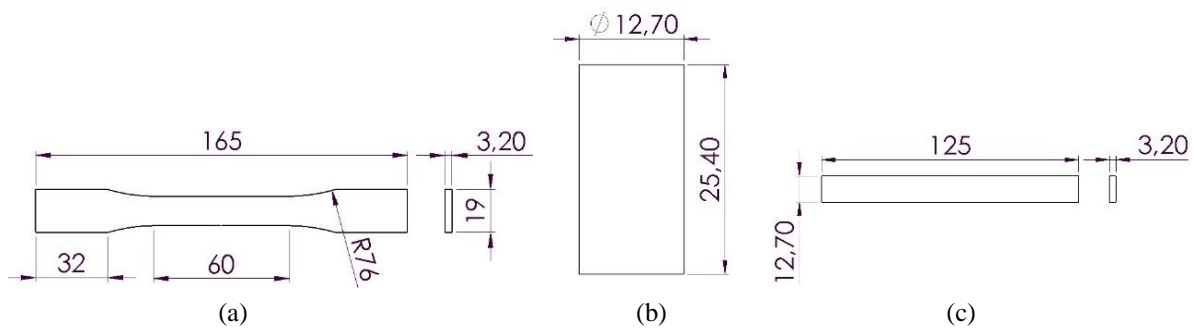


Figure 2. Dimensions of test specimens in ASTM standards (mm) (a) Tensile specimen (b) Compression specimen (c) 3-point bending specimen

2.2 Methods

In this section, the fabrication process of tensile, compression and bending test samples is given. The printing parameters of SLA and FDM-based printers must be adjusted for fabrication with 3D printers. The printing parameters selected for ABS, PLA, and UVR materials. Although the occupancy rate was chosen as fixed in both printers, other parameters had to be selected differently because there were different types of printers. In addition, since the printing temperature values materials are different in FDM technique, two nozzle and table temperatures were determined.

The parameters in Table 2 are defined in the slicing program of the 3D printer to generate the G-codes of the solid modelled samples. This code defines settings such as the position and angle of the part to be printed on the printer table. The G-codes fabricated in the program are transferred to the 3D printer with the help of a USB, and the part is made ready for printing. The printer table needs to be calibrated manually for both 3D printers. After this process, the necessary material is attached to the printer or poured, and fabrication is started. Before starting the manufacturing process, a thin film of adhesive was applied to the print bed in the FDM method to ensure better adhesion of the first layer of the sample to the glass print bed during fabrication.

Table 2. 3D printing parameters used in FDM and SLA methods.

| | Fill Rate (%) | Layer Thickness (mm) | Wall Thickness (mm) | Print Speed (mm/s) | Nozzle Temperature (°C) | Table Temperature (°C) |
|-----|---------------|----------------------|-----------------------|--------------------|-----------------------------|------------------------|
| FDM | 75 | 0.15 | 0.9 | 50 | 200/220 | 70/80 |
| | Fill Rate (%) | Layer Thickness (mm) | Number of Base Layers | Print Speed (mm/s) | Number of Transition Layers | Exposure Time (s) |
| SLA | 75 | 0.03 | 15 | 1.8 | 10 | 80 |

Calibration settings were made on the FDM 3D printer, and the red color Creality, brand PLA material, was attached to the printer for the fabrication of tensile test specimens. The samples were fabricated according to the parameters in Table 2 as in Figure 3a. The same print settings were repeated, and the fabrication was made with yellow Creality brand ABS material. Ten tensile specimens were fabricated by the FDM method, five for each material type. Finally, the tensile samples in Figure 3a were fabricated on an SLA-based printer using transparent Anycubic brand UVR material. Thus, fifteen tensile test specimens were fabricated following ASTM D638-14 standards with three materials and two different fabrication techniques. Using the same printing parameters and material types, fifteen 3-point bending test specimens were fabricated in ASTM D790 standards as in Figure 3b. Finally, fifteen compression test samples were fabricated in accordance with ASTM D695 standards as in Figure 4.



Figure 3. Tensile and 3-point bending test specimens fabricated on a 3D printer using PLA, ABS and UVR materials: (a) Tensile test specimens (b) 3-point bending test specimens



Figure 4. Compression test samples fabricated on a 3D printer using PLA, ABS and UVR materials

3. RESULTS AND DISCUSSION

Mechanical test sample groups fabricated by FDM and SLA additive manufacturing methods are named according to the mechanical tests to be applied. The tensile test sample group is named the letter 'T', the compression test sample group is named the letter 'C', and the 3-point bending test sample group is named 'B'. The results are given both graphically and in tabular form.

3.1 Tensile Strength Tests Results

Tensile experimental studies were performed on a 50 kN capacity test device (AG-X, Shimadzu) using the ASTM D638-14 standard. The device has a reading range of $\pm 0.1\%$ between 50kN and 50N according to ISO 7500/1, ASTM E4, and DIN51221 standards. The test speed range is 0.0005mm/min-1000mm/min. Experimental studies were carried out at a tensile speed of 1 mm/s. The stress-strain diagrams resulting from the tensile test of the samples fabricated with PLA, ABS, and UVR materials are shown in Figure 5. The stress, percent elongation, and modulus of elasticity calculated according to the applied force and elongation are given in Table 3.

Table 3. Tensile test results of PLA, ABS and UVR materials

| PLA | Strength (MPa) | Strain (%) | Elasticity Module (GPa) | ABS | Strength (MPa) | Strain (%) | Elasticity Module (GPa) | UVR | Strength (MPa) | Strain (%) | Elasticity Module (GPa) |
|----------------|----------------|------------|-------------------------|------------|----------------|------------|-------------------------|------------|----------------|------------|-------------------------|
| T1 | 36.12 | 2.48 | 1.452 | T1 | 25.75 | 2.37 | 1.084 | T1 | 61.75 | 4.39 | 1.403 |
| T2 | 36.42 | 2.26 | 1.592 | T2 | 27.74 | 2.42 | 1.114 | T2 | 54.42 | 3.72 | 1.627 |
| T3 | 36.51 | 2.19 | 1.716 | T3 | 28.72 | 2.44 | 1.117 | T3 | 61.31 | 4.48 | 1.366 |
| T4 | 36.21 | 2.35 | 1.552 | T4 | 31.65 | 2.43 | 1.319 | T4 | 62.36 | 4.47 | 1.391 |
| T5 | 36.73 | 2.49 | 1.478 | T5 | 32.81 | 2.44 | 1.332 | T5 | 62.14 | 4.27 | 1.453 |
| Average | 36.39 | 2.35 | 1.558 | | 29.33 | 2.42 | 1.193 | | 60.39 | 4.26 | 1.448 |

The highest tensile strength value occurs in the samples fabricated with the SLA technique using UVR material. When Figure 5 is examined, it can be said that the strength-strain curves of the samples fabricated using different materials coincide. When the strength-strain curves of the products fabricated with UVR and ABS materials are compared, the tensile strength values of the products fabricated with UVR material are approximately 90% higher than those fabricated with ABS material. The elongation at break values of the products fabricated with ABS material is 60% higher than those fabricated with UVR material. This is because the bond structure between the layers in the 3D printing process is better in UVR material samples than in PLA and ABS materials. The average elongation amounts of PLA, ABS, and UVR samples were determined as 2.35 mm, 2.42 mm, and 4.26 mm, respectively. The mean modulus of elasticity values of PLA, ABS, and UVR material samples was calculated as 1.558 GPa, 1.193 GPa, and 1.448 GPa, respectively.

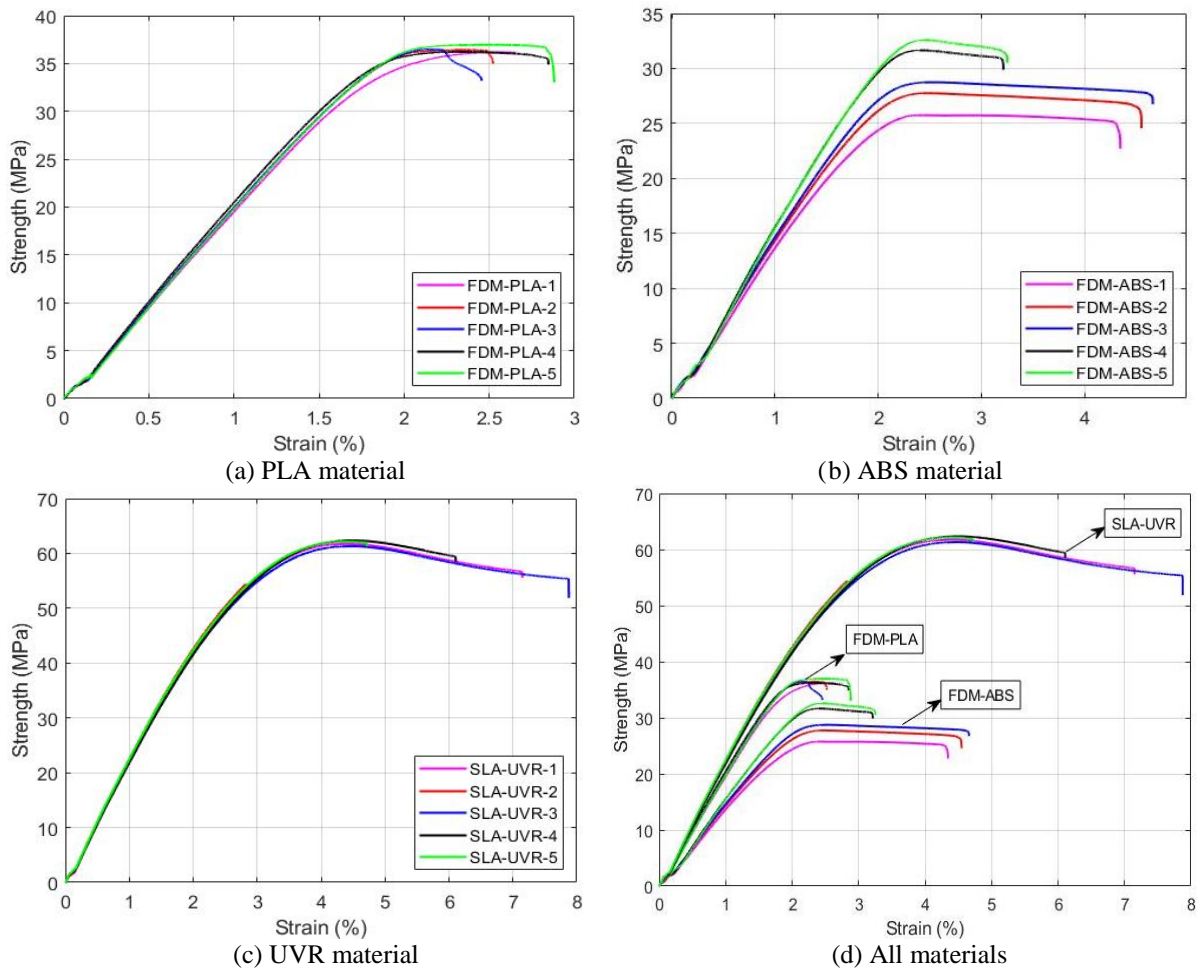


Figure 5. Strength-strain diagrams of tensile tests for tensile specimens made of different materials (a) PLA materials (b) ABS materials (c) UVR materials (d) All materials

The tensile strength of the samples fabricated by the SLA method is higher than FDM because they have isotropic properties. With this feature, SLA-type specimens have the same force value in all directions. When the tensile and elasticity modulus data obtained as a result of the tensile test and the existing studies in the literature are examined, it is seen that there is a similarity in terms of material properties. Zhao et al. (Zhao et al., 2019) investigated the effect of compression angle and layer thickness on the tensile strength and Young's modulus of PLA materials fabricated with FDM. According to the results, the printing material with a 90° compression angle and 0.1 mm layer thickness had the highest tensile strength with 49.66 MPa. In contrast, the printing material with 0° compression angle and 0.3 mm layer thickness had the highest tensile strength with 19.16 MPa. Grabowik et al. (Grabowik et al., 2017) presented tensile test results for samples from ABS, PLA, PET, PMMA, ASA, and wood material groups. The peak stress value for ABS material is between 34.6 and 35 MPa.

3.2 Compression Tests Results

Compression test experimental studies were performed on a 50 kN capacity test device (AG-X, Shimadzu) using the ASTM D695 standard. The study applied a constantly increasing compression load to PLA, ABS, and UVR material samples placed between two jaws. The stress-strain diagrams resulting from the compression test applied to the specimens are given in Figure 6. The stress, percent elongation, and modulus of elasticity calculated according to the applied force and elongation are given in Table 4.

Table 4. Compression test results of PLA, ABS and UVR materials

| PLA | Strength (MPa) | Strain (%) | Elasticity Module (GPa) | ABS | Strength (MPa) | Strain (%) | Elasticity Module (GPa) | UVR | Strength (MPa) | Strain (%) | Elasticity Module (GPa) |
|----------------|----------------|------------|-------------------------|------------|----------------|------------|-------------------------|------------|----------------|------------|-------------------------|
| C1 | 94.63 | 6.63 | 0.601 | C1 | 86.56 | 6.51 | 0.531 | C1 | 130.02 | 2.90 | 1.752 |
| C2 | 93.57 | 6.51 | 0.602 | C2 | 88.66 | 6.44 | 0.538 | C2 | 131.42 | 3.06 | 1.685 |
| C3 | 93.82 | 6.74 | 0.603 | C3 | 88.52 | 6.68 | 0.528 | C3 | 116.12 | 2.35 | 1.945 |
| C4 | 94.12 | 6.52 | 0.592 | C4 | 88.42 | 6.64 | 0.529 | C4 | 127.54 | 2.93 | 1.712 |
| C5 | 95.15 | 6.73 | 0.598 | C5 | 88.75 | 6.56 | 0.536 | C5 | 133.62 | 3.02 | 1.743 |
| Average | 94.25 | 6.62 | 0.599 | | 88.18 | 6.56 | 0.532 | | 127.74 | 2.85 | 1.767 |

The UVR material samples have higher compressive strength values than ABS and PLA samples (Figure 6). The most important factor affecting compressive strength is the material's molecular structure. The differences in the molecular structures of the materials used in the test processes, the chemical composition, metallographic structure, and the number of functional groups of the polymers affected the compressive strength. The UVR material structure consists of resin + photoinitiators. Photoinitiators absorb light of different wavelengths and form free radicals that initiate crosslinking and curing of a formula. Among the process parameters, the elastic range of ABS material is minimal and visible for UVR and PLA. Taking the average of the experimental studies, the compressive strengths for PLA, ABS, and UVR were calculated as 94.25 MPa, 88.18 MPa, and 127.74 MPa, respectively. The mean modulus of elasticity values of PLA, ABS, and UVR material samples was calculated as 0.599 GPa, 0.532 GPa, and 1.767 GPa, respectively.

When the strength data obtained as a result of the compression test and the existing studies in the literature are examined, it is seen that there is a similarity in terms of material properties. Kholil et al. (Kholil et al., 2022) aimed to determine the compressive strength of FDM with parameters. The sample fabrication process includes ABS and PLA materials. The highest compressive strength was found in PLA material with a yield strength value of 66.78 MPa and a layer thickness of 0.15 mm. The lowest compressive strength was found in ABS material, with a yield strength value of 33.41 MPa and a layer thickness of 0.35 mm. Miedzińska et al. (Miedzińska et al., 2020) present the results of durability tests on selected materials used for printing with SLA technology. To determine the properties of these materials, two types of tests differing in strain rate were used: the quasistatic test on the Zwick & Roell Kappa 50DS strength machine and the dynamic test on the Hopkinson bar. As a result of the experimental studies performed with Tough and Clear type resins, the average values of the maximum compressive strength were found to be 189.5 MPa and 231.2 MPa, respectively. The strain ratios at these values were measured as 4.568 and 5.994. Based on the results obtained, the tested Tough and Clear light-curable resins revealed that the strain rate significantly affected the compressive behaviour, yield strength, material weakening, and strain hardening. Static compression tests revealed the elastic-plastic behaviour of the material. The 50% of strains obtained in the tests did not cause cracking in the samples. The samples were deformed but remained consistent.

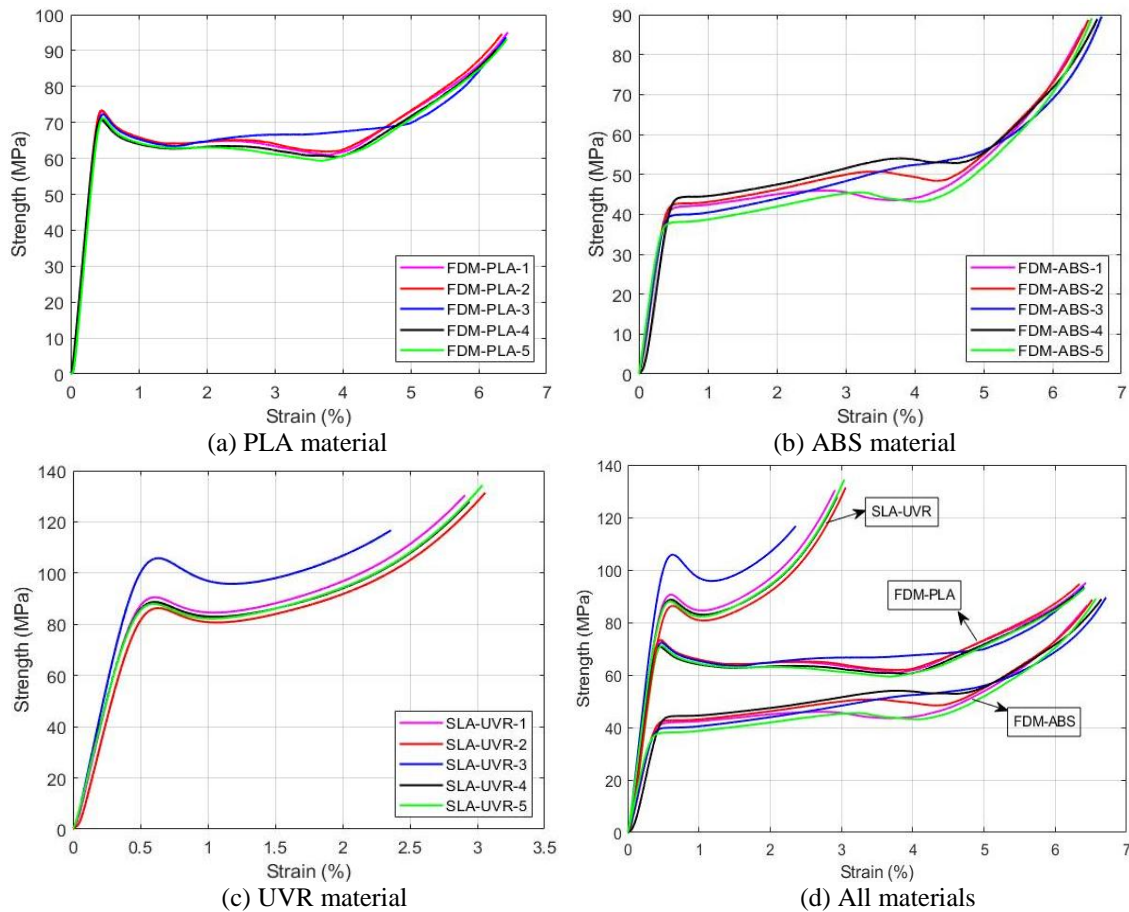


Figure 6. Strength-strain diagrams of compression tests for compression specimens made of different materials (a) PLA materials (b) ABS materials (c) UVR materials (d) All materials

3.3 3-Point Bending Tests Results

The 3-point bending test is usually performed on brittle materials rather than a tensile test. For this reason, the 3-point bending test gives more meaningful results in brittle materials. Bend test studies were performed on a 50 kN force transducer capacity machine (AGS-X, Shimadzu) using the ASTM D790 standard. The mandrel's diameter and the supports' diameter were fixed in accordance with the standard. After the assemblies were fixed, both PLA, ABS, and UVR materials were placed on the supports for the test specimens, and the specimens were bent with the help of a mandrel by applying the load. The strength-strain diagrams resulting from the 3-point bending test of the samples are shown in Figure 7. The stress, percent elongation, and modulus of elasticity calculated according to the applied force and elongation are given in Table 5.

Table 5. 3-point bending test results of PLA, ABS and UVR materials

| PLA | Strength (MPa) | Strain (%) | Elasticity Module (GPa) | ABS | Strength (MPa) | Strain (%) | Elasticity Module (GPa) | UVR | Strength (MPa) | Strain (%) | Elasticity Module (GPa) |
|----------------|----------------|------------|-------------------------|-----------|----------------|------------|-------------------------|-----------|----------------|------------|-------------------------|
| B1 | 78.35 | 3.26 | 0.913 | B1 | 37.57 | 3.44 | 0.406 | B1 | 117.91 | 2.72 | 1.205 |
| B2 | 80.60 | 3.12 | 0.881 | B2 | 56.72 | 3.43 | 0.621 | B2 | 120.22 | 3.03 | 1.214 |
| B3 | 80.28 | 2.87 | 0.901 | B3 | 44.82 | 3.42 | 0.493 | B3 | 121.34 | 3.32 | 1.195 |
| B4 | 80.68 | 3.44 | 0.865 | B4 | 54.18 | 3.39 | 0.598 | B4 | 118.38 | 2.95 | 1.186 |
| B5 | 80.01 | 3.15 | 0.910 | B5 | 53.45 | 3.44 | 0.615 | B5 | 113.92 | 3.43 | 1.198 |
| Average | 79.98 | 3.16 | 0.894 | | 49.34 | 3.42 | 0.546 | | 118.35 | 3.09 | 1.199 |

The highest bending strength was observed in the samples made of UVR material. The lowest bending moment was found in ABS materials. The average bending strength values for PLA, ABS, and UVR samples were 79.98 MPa, 49.34 MPa, and 118.35 MPa, respectively. It can be seen that results similar to the compression test were obtained. The most important reason for this is the difference between the molecular structure of the materials. In addition, the high bending strength of the UVR material led to higher bending strength values.

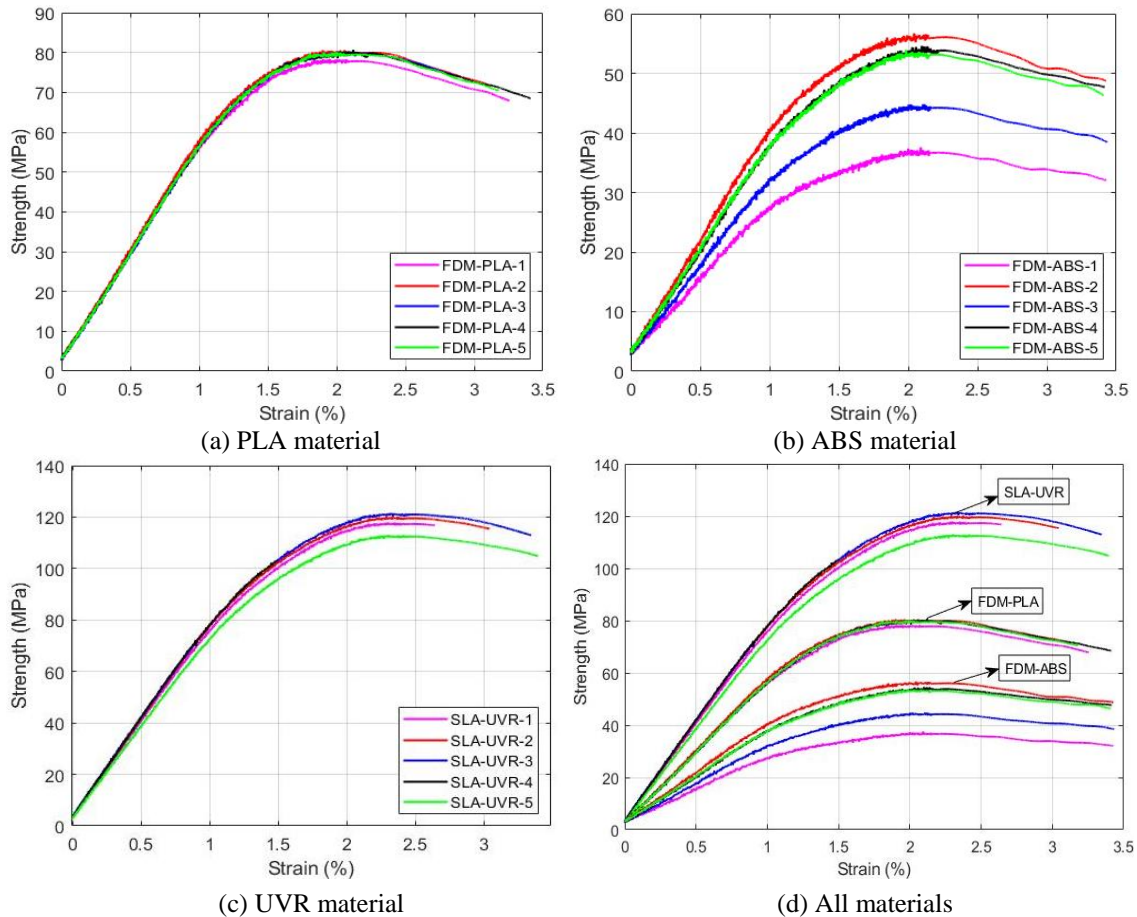


Figure 7. Strength-strain diagrams of 3-point bending tests for 3-point bending specimens made of different materials (a) PLA materials (b) ABS materials (c) UVR materials (d) All materials

This bending strength was followed by PLA and ABS materials, respectively. While the bending strength values of UVR and PLA samples were close to each other for five tests; there are 25% differences in ABS materials. The elastic range is visible for all materials. When the average of the experimental studies is taken, the percent elongation values for PLA, ABS, and UVR materials were calculated as 3.16%, 3.42%, and 3.09%, respectively. The mean modulus of elasticity values of PLA, ABS, and UVR material samples was calculated as 0.894 GPa, 0.546 GPa, and 1.199 GPa, respectively.

When the data obtained as a result of the 3-point bending test and the existing studies in the literature are examined, it is seen that there is a similarity in terms of material properties. Atakok et al. (Atakok et al., 2022) used the Taguchi methodology to investigate the effects of FDM fabrication parameters (tensile strength, three-point flexural strength, and 3D-printed PLA and Re-PLA) on impact strength. Filaments (PLA, Re-PLA), three different layer thicknesses, filling ratios, and filling structure were determined as FDM process parameters.

3.4 Hardness Measurement Results

Hardness measurements of the test sample were made with the TRONIC PD-801 Analog Shoremeter device in SHORE D. The Shoremeter device is suitable for measuring hard rubber, synthetic materials, thermoplastics, vinyl sheets, cellulose acetates and MDF. Tensile test sample was used for hardness measurements. Hardness measurements were made from 5 different points on the upper and lower surfaces of each sample and calculations were made by taking the average values. The measured hardness values are given in Table 6. When the test samples fabricated with PLA, ABS and UVR materials are compared among themselves, it is seen that the hardness values of the products fabricated with UVR material are higher than the products. Made from PLA and ABS. The reason for this is that the void structure in products fabricated with UVR is quite low compared to other materials. When the upper and lower zone hardness values are examined, it is seen that the lower surface hardness is higher than the upper surface hardness. It is thought that the adhesives applied to ensure the adhesion of the sample to the glass table in the manufacturing made with the FDM technique cause the hardness of the lower surfaces of the samples to increase. For this reason, the substrate hardness of ABS and PLA samples was higher. Similarly, the hardness of the sample fabricated with the SLA technique was higher on the surface that first adhered to the table, that is, the lower surface.

Table 6. Hardness values of PLA, ABS and UVR materials

| | Shore D Hardness Values | |
|------------|-------------------------|------------------------|
| | Top Surface Average | Bottom Surface Average |
| PLA | 62.15 | 75.13 |
| ABS | 69.77 | 80.35 |
| UVR | 72.54 | 84.76 |

3.5. Surface Analysis Results

Surface image analysis was performed with a scanning electron micro-scope (SEM) device to examine the surface morphology of the tensile test specimens fabricated from PLA, ABS, and UVR materials after breaking within the scope of experimental studies. With SEM, besides taking surface images at high magnifications, information about the chemical composition of the material can also be obtained. Images of the fractured areas of the specimens broken in the tensile tests were taken with the ZEISS Gemini 500 FESEM.

After the tensile test was applied to PLA, ABS, and UVR materials, pictures of the fractured areas of the fracture test specimens were taken in the SEM device with 40x, 100x, 2000x, and 5000x magnifications and are given in Figure 8. SEM analysis of the UVR test sample shows that the material interface is better compared to ABS and PLA samples. It is seen in Figure 8f that there is almost no gap in each layer of the sample fabricated with UVR material. The gaps between the 3D printed fibers in each layer of the fabricated samples are higher in ABS samples (Figure 8g). In the 5000x magnified images of the fracture areas of the fabricated samples in SEM, it is seen that the interlayer gaps in the ABS sample are much larger. The sample's hardening and strength are reduced by its extensive void structure. When the samples fabricated with ABS and PLA are examined, it is seen that the 3D-printed fibres in each layer are in linear contact with each other (Figure 8a and Figure 8b).

It can be said that the ABS material test sample behaves like a ductile material because the interlayer bonds are weaker. Surface fractures of PLA and UVR materials indicate a brittle fracture.

Although it seems to be a partially brittle fracture in ABS material, it exhibited a slightly different fracture behaviour as it has a hollower structure. In the SEM image of the PLA sample in Figure 8e, up to half of the material is where the fracture starts and where the fracture is very rapid and brittle. Later, as the shrinkage continued, the lower part of the material was catastrophically broken, and a wavy structure was formed. The UVR material also appears to have a very brittle fracture.

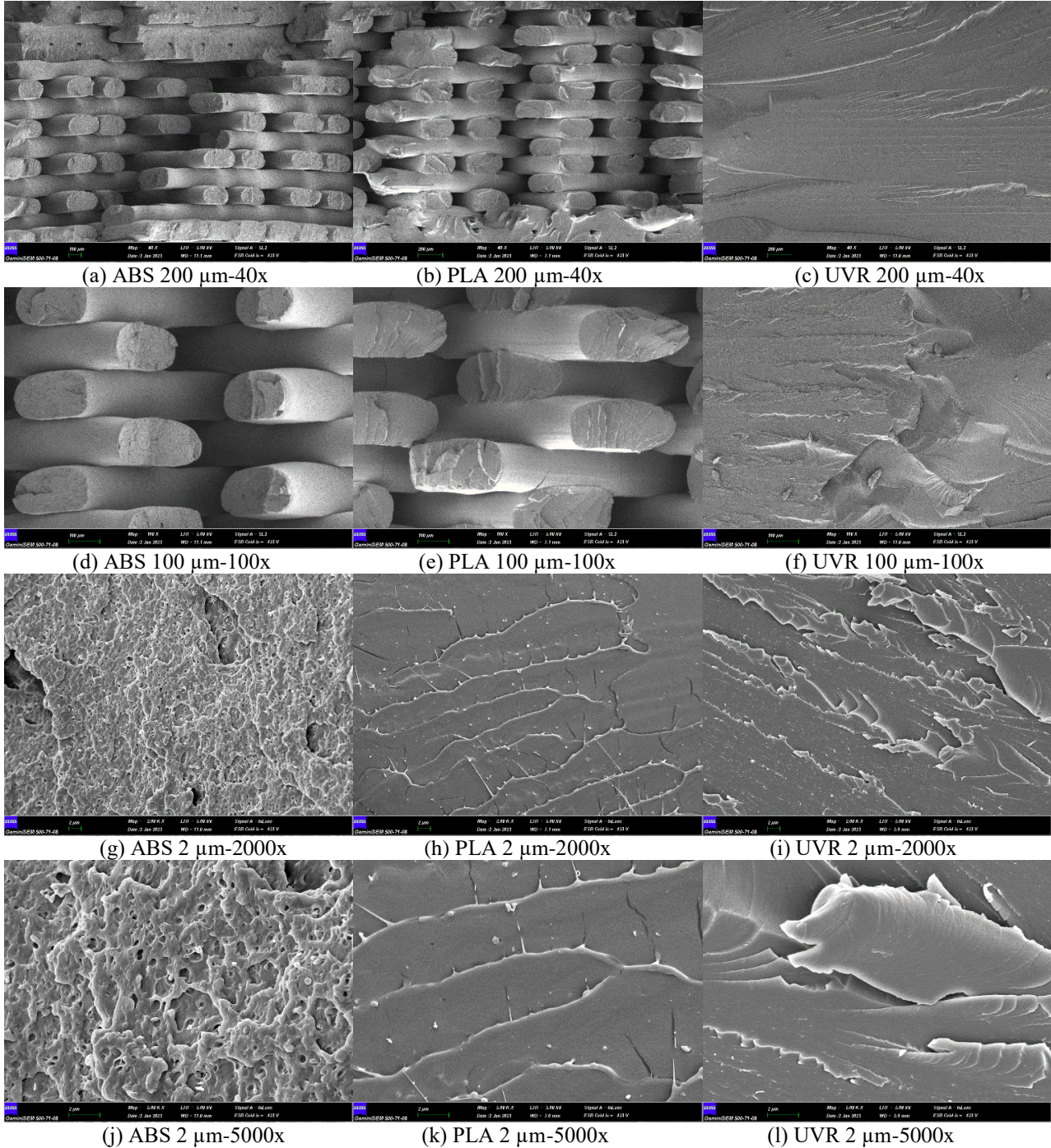


Figure 8. 40x, 100x, 2000x and 5000x magnified images taken from SEM of the broken parts of the samples as a result of the tensile test (a) ABS 200 μm -40x (b) PLA 200 μm -40x (c) UVR 200 μm -40x (d) ABS 100 μm -100x (e) PLA 100 μm -100x (f) UVR 100 μm -100x (g) ABS 2 μm -2000x (h) PLA 2 μm -2000x (i) UVR 2 μm -2000x (j) ABS 2 μm -5000x (k) PLA 2 μm -5000x (l) UVR 2 μm -5000x

4. CONCLUSION

This study fabricated tensile, compression, and 3-point bending test specimens following the standards using PLA, ABS, and UVR-type materials with FDM and SLA-based additive manufacturing methods. The mechanical properties of these materials were examined and compared with the tests performed. For each material type, fifteen test specimens were fabricated. ASTM standard was used for sizing forty-five test samples fabricated with a 3D printer. PLA, ABS, and UVR is important for efficient parts operation and the widespread use of the fabrication technique. The best mechanical properties were observed in the test specimens made of UVR material. The highest tensile, compressive, and bending strengths were measured in these samples. These values are, on average, 60.39 MPa, 127.74 MPa, and 118.35 MPa, respectively. After the UVR material, the highest strength values were observed in the PLA sample, while the lowest values were measured in the ABS samples. When the test samples fabricated with PLA, ABS, and UVR materials are compared among themselves, it is seen that the hardness values of the products fabricated with UVR material are higher than the products fabricated with PLA and ABS. This is because the void structure inside the UVR samples is very small compared to other materials. Finally, surface image analysis was performed with the SEM device to examine the surface morphology fabricated from PLA, ABS, and UVR materials after breaking. As a result of the analysis, the excess of the void structure and the bond weakness in the ABS samples were observed.

5. ACKNOWLEDGEMENTS

This work is supported by the Scientific Research Projects Coordination Unit of Siirt University as a project with the number 2022-SİÜMÜH-009. This study was carried out in the Additive Manufacturing and Seismic Isolator Laboratory of the Siirt University Faculty of Engineering. The author of this article would like to thank the staff of the Additive Manufacturing and Seismic Isolator Laboratory for their support.

6. CONFLICT OF INTEREST

Authors approve that to the best of their knowledge, there is not any conflict of interest or common interest with an institution/organization or a person that may affect the review process of the paper.

7. AUTHOR CONTRIBUTION

Conceptualization, M. Said Bayraklılar and Melih Kuncan; Methodology, Osman Ulkir and Melih Kuncan; Formal analysis, M. Said Bayraklılar and Abdulkadir Buldu; Investigation, M. Tayyip Kocak and Osman Ulkir; Validation, M. Tayyip Kocak and Melih Kuncan; Software, Abdulkadir Buldu, M. Tayyip Kocak and Osman Ulkir; Data curation, M. Said Bayraklılar and Melih Kuncan; Writing-original draft and review & editing, M. Said Bayraklılar, Abdulkadir Buldu and Osman Ulkir.

8. REFERENCES

- Aloyaydi B. A., Sivasankaran S., Low-velocity impact characteristics of 3D-printed poly-lactic acid thermoplastic processed by fused deposition modeling. *Transactions of the Indian Institute of Metals* 73, 1669-1677, 2020
- Atakok G., Kam, M., Koc H.B., Tensile, three-point bending and impact strength of 3D printed parts using PLA and recycled PLA filaments: A statistical investigation. *Journal of Materials Research and Technology* 18, 1542-1554, 2022.
- Ble-Bail A., Maniglia B.C., Le-Bail P., Recent advances and future perspective in additive manufacturing of foods based on 3D printing. *Current Opinion in Food Science* 35, 54-64, 2020.
- Böckin D., Tillman A.M., Environmental assessment of additive manufacturing in the automotive industry. *Journal of cleaner production*, 226, 977-987, 2019.
- Camargo J.C., Machado Á.R., Almeida E.C., Silva E.F.M.S., Mechanical properties of PLA-graphene filament for FDM 3D printing. *The International Journal of Advanced Manufacturing Technology* 103, 2423-2443, 2019.
- Chacón J.M., Caminero M.A., García-Plaza E., Núñez P.J., Additive manufacturing of PLA structures using fused deposition modelling: Effect of process parameters on mechanical properties and their optimal selection. *Materials & Design* 124, 143-157.
- Chaudhary R., Fabbri P., Leoni E., Mazzanti F., Akbari R., Antonini C., Additive manufacturing by digital light processing: a review. *Progress in Additive Manufacturing* 8, 331-351, 2023.
- Cheng B., Shrestha S., Chou, K., Stress and deformation evaluations of scanning strategy effect in selective laser melting. *Additive Manufacturing* 12, 240-251, 2016.
- Chesser P., Post B., Roschli A., Carnal C., Lind R., Borish M., Love L., Extrusion control for high quality printing on Big Area Additive Manufacturing (BAAM) systems. *Additive Manufacturing* 28, 445-455, 2019.
- Chohan J.S., Singh R., Pre and post processing techniques to improve surface characteristics of FDM parts: a state of art review and future applications. *Rapid Prototyping Journal* 23, 495-513, 2017.
- De León A.S., Domínguez-Calvo A., Molina S.I., Materials with enhanced adhesive properties based on acrylonitrile-butadiene-styrene (ABS)/thermoplastic polyurethane (TPU) blends for fused filament fabrication (FFF). *Materials & Design* 182, 108044, 2019.
- Dehurtevent M., Robberecht L., Hornez J.C., Thuault A., Deveaux E., Béhin P., Stereolithography: A new method for processing dental ceramics by additive computer-aided manufacturing. *Dental materials* 33, 477-485, 2017.
- Du Plessis A., Yadroitsava I., Yadroitsev I., Effects of defects on mechanical properties in metal additive manufacturing: A review focusing on X-ray tomography insights 2020, *Materials & Design* 187, 108385, 2020.
- Duman B., Özsoy K., A deep learning-based approach for defect detection in powder bed fusion additive manufacturing using transfer learning. *Journal of the Faculty of Engineering and Architecture of Gazi University* 37, 361-375, 2022.
- Ertugrul I., Ulkir O., Ersoy S., Ragulskis M., Additive Manufactured Strain Sensor Using Stereolithography Method with Photo-polymer Material. *Polymers* 15, 991, 2023.
- Galati M., Iuliano L., A literature review of powder-based electron beam melting focusing on numerical simulations. *Additive Manufacturing* 19, 1-20, 2018.
- Grabowik C., Kalinowski K., Ćwikła G., Paprocka I., Kogut P., Tensile tests of specimens made of selected group of the filament materials manufactured with FDM method. In *MATEC Web of Conferences* 112, 04017, 2017.

- Haleem A., Javaid M., Additive manufacturing applications in industry 4.0: a review. *Journal of Industrial Integration and Management* 4, 1930001, 2019.
- Heidari-Rarani M., Rafiee-Afarani M., Zahedi A.M., Mechanical characterization of FDM 3D printing of continuous carbon fiber reinforced PLA composites. *Composites Part B: Engineering* 175, 107147, 2019.
- Ishak M. R., Leman Z., Sapuan S. M., Edeerozey A. M. M., Othman I. S., Mechanical properties of kenaf bast and core fibre reinforced unsaturated polyester composites. In *IOP Conference Series: Materials Science and Engineering* 11 (1), 012006, 2010.
- Kafle A., Luis E., Silwal R., Pan H.M., Shrestha P.L., Bastola A.K., 3D/4D Printing of polymers: Fused deposition modelling (FDM), selective laser sintering (SLS), and stereolithography (SLA). *Polymers* 13, 3101, 2021.
- Kawalkar R., Dubey H.K., Lokhande S.P., A review for advancements in standardization for additive manufacturing. *Materials Today: Proceedings* 50, 1983-1990, 2022.
- Kempin W., Franz C., Koster L.C., Schneider F., Bogdahn M., Weitschies W., Seidlitz A., Assessment of different polymers and drug loads for fused deposition modeling of drug loaded implants. *European Journal of Pharmaceutics and Biopharmaceutics* 115, 84-93, 2017.
- Kholil A., Asyaefudin E., Pinto N., Syaripuddin S., Compression Strength Characteristics of ABS and PLA Materials Affected by Layer Thickness on FDM. In *Journal of Physics: Conference Series* 2377, 012008, 2022.
- Kim Y., Choi E. S., Kwak W., Shin Y., Analysis of the thermal distribution by using laser-beam irradiation. *Journal of the Korean Physical Society* 51, 503-508, 2007.
- Laureto J. J., Pearce J. M., Anisotropic mechanical property variance between ASTM D638-14 type i and type iv fused filament fabricated specimens. *Polymer Testing*, 68, 294-301, 2018.
- Li W., Mille L.S., Robledo J.A., Uribe T., Huerta V., Zhang Y.S., Recent advances in formulating and processing biomaterial inks for vat polymerization-based 3D printing. *Advanced healthcare materials* 9, 2000156, 2020.
- Marşavina L., Vălean C., Mărghitaş M., Linul E., Razavi N., Berto F., Brighenti R., Effect of the manufacturing parameters on the tensile and fracture properties of FDM 3D-printed PLA specimens. *Engineering Fracture Mechanics* 274, 108766, 2022.
- Mercado-Colmenero J.M., La Rubia M.D., Mata-Garcia E., Rodriguez-Santiago M., Martin-Doñate C., Experimental and numerical analysis for the mechanical characterization of petg polymers manufactured with FDM technology under pure uniaxial compression stress states for architectural applications. *Polymers* 12, 2202, 2020.
- Miedzińska D., Gielet R., Małek E., Experimental study of strength properties of SLA resins under low and high strain rates. *Mechanics of Materials* 141, 103245, 2020.
- Morão A., De Bie, F., Life cycle impact assessment of polylactic acid (PLA) produced from sugarcane in Thailand. *Journal of Polymers and the Environment*, 27(11), 2523-2539, 2019.
- Mukhtarkhanov M., Perveen A., Talamona D., Application of stereolithography based 3D printing technology in investment casting. *Micromachines* 11, 946, 2020.
- Nguyen A.K., Narayan, R.J., Two-photon polymerization for biological applications. *Materials Today* 20, 314-322, 2017.
- Özsoy K., Aksoy B., Bayrakçı H.C., Optimization of thermal modeling using machine learning techniques in fused deposition modeling 3-D printing. *Journal of Testing and Evaluation* 50, 613-628, 2022.

- Özsoy K., Erçetin A., Çevik Z.A., Comparison of mechanical properties of PLA and ABS based structures fabricated by fused deposition modelling additive manufacturing. *Avrupa Bilim ve Teknoloji Dergisi* 27, 802-809, 2021.
- Patpatiy P., Chaudhary K., Shastri A., Sharma S., A review on polyjet 3D printing of polymers and multi-material structures. *Proceedings of the Institution of Mechanical Engineers, Part C: Journal of Mechanical Engineering Science* 236, 7899-7926, 2022.
- Prabhakar M.M., Saravanan A.K., Lenin A.H., Mayandi K., Ramalingam P.S., A short review on 3D printing methods, process parameters and materials. *Materials Today: Proceedings* 45, 6108-6114, 2021.
- Salman S. D., Hassimb W. W., Leman Z, Experimental comparison between two types of hybrid composite materials in compression test. *Carbon*, 3, 119-23, 2015.
- Shassere B., Nycz A., Noakes M.W., Masuo C., Sridharan N., Correlation of microstructure and mechanical properties of metal big area additive manufacturing. *Applied Sciences* 9, 787, 2019.
- Shi K., Salvage J.P., Maniruzzaman M., Nokhodchi A., Role of release modifiers to modulate drug release from fused deposition modelling (FDM) 3D printed tablets. *International journal of pharmaceutics* 597, 120315, 2021.
- Singh S., Ramakrishna S., Singh R., Material issues in additive manufacturing: A review. *Journal of Manufacturing Processes* 25, 185-200, 2017.
- Turan S. R., Ülker O., Kuncan M., Buldu A., Stereolithografi eklemeli imalat yöntemiyle farklı doluluk oranlarında üretilen numunelerin mekanik özelliklerinin incelenmesi. *International Journal of 3D Printing Technologies and Digital Industry* 6(3), 399-407.
- Uludag M., Ulkir O., Ertugrul, I., Kaplanoglu E., Design, fabrication, and experiments of a soft pneumatic gripper with closed-loop position control. *Journal of Testing and Evaluation* 51, 2023.
- Yadav D., Chhabra D., Garg R.K., Ahlawat A., Phogat A., Optimization of FDM 3D printing process parameters for multi-material using artificial neural network. *Materials Today: Proceedings* 21, 1583-1591, 2020.
- Yadav D.K., Srivastava R., Dev S., Design & fabrication of ABS part by FDM for automobile application. *Materials Today: Proceedings* 26, 2089-2093, 2020.
- Yang Y., Li L., Zhao J., Mechanical property modeling of photosensitive liquid resin in stereolithography additive manufacturing: Bridging degree of cure with tensile strength and hardness. *Materials & Design* 162, 418-428, 2019.
- Zhao Y., Chen Y., Zhou Y., Novel mechanical models of tensile strength and elastic property of FDM AM PLA materials: Experimental and theoretical analyses. *Materials & Design* 181, 108089, 2019.